PHYSICAL REVIEW D **91,** 035029 (2015)

Dark matter at the pseudoscalar Higgs resonance in the phenomenological MSSM and SUSY GUTs

Archana Anandakrishnan,[1,*] Bibhushan Shakya,[2,†] and Kuver Sinha[3,‡]

[1]*Department of Physics, The Ohio State University*
191 West Woodruff Avenue, Columbus, Ohio 43210, USA
[2]*Michigan Center for Theoretical Physics University of Michigan, Ann Arbor, Michigan 48109, USA*
[3]*Department of Physics, Syracuse University Syracuse, New York 13244, USA*

(Received 16 December 2014; published 26 February 2015)

We study dark matter at the MSSM pseudoscalar Higgs resonance (A funnel), which is one of the few remaining MSSM thermal dark matter candidates in the 100–1000 GeV range safe from direct detection constraints. To illustrate the various factors at play, this study is performed in two contrasting setups: a bottom-up phenomenological MSSM (pMSSM) approach that allows significant freedom and the top-down, highly constrained Yukawa unified $SO(10)$ GUT model. In the pMSSM, for $\mu > 0$, the entire parameter space lies above the coherent neutrino background and mostly within reach of XENON1T and LZ, while blind spots exist at $m_A > 800$ GeV for $\mu < 0$; the strongest constraints come from $A/H \to \tau\tau$ searches at the LHC. For Yukawa unified models, the confluence of $B_s \to \mu^+\mu^-$ constraints, fits to the bottom quark and Higgs masses, and gluino mass bounds from the LHC result in a prediction: realizing the pseudoscalar resonance *requires* gaugino mass nonuniversality, with a mass ratio that is determined to within a small range.

DOI: 10.1103/PhysRevD.91.035029 PACS numbers: 12.60.Jv, 95.35.+d

I. INTRODUCTION

Since the weak scale presumably holds the key to a host of pressing theoretical questions such as the exact nature and naturalness of electroweak symmetry breaking, the WIMP miracle—the thermal production of a particle with weak-scale mass and interactions in the early Universe matches the observed dark matter relic abundance—has long served as a conduit between particle physics model building and dark matter cosmology and as a target for colliders and direct detection experiments. Central to dark matter model building is the paradigm of supersymmetry, since it comes with its own strong motivations. The most well-studied model of supersymmetry is the minimal one (MSSM), which looks to be increasingly fine-tuned in view of the nonobservation of superpartners at the LHC. Cherished simple parametrizations such as the CMSSM or mSUGRA have either been ruled out or pushed into remote corners, and full phenomenological studies of the MSSM (pMSSM) have been undertaken.

The WIMP miracle is realized in the MSSM with the lightest neutralino as the lightest supersymmetric particle (LSP); however, there now exist significant constraints on such a thermal dark matter candidate. Increasingly stringent direct detection bounds, most recently from XENON-100 [1] and LUX [2] are rapidly cutting into the parameter space of supersymmetry, particularly that of well-tempered neutralinos [3], requiring fine-tuning to evade such constraints [4,5]. A pure Higgsino or wino LSP with annihilation mainly to gauge boson final states can evade such constraints; however, these candidates are constrained by indirect detection [6–9]. Coannihilation (with slepton, sfermion, chargino, or heavier neutralino) can also result in the correct relic density, but involve a light state close to the LSP mass with stronger interactions that can be probed experimentally.

The purpose of this paper is to study the prospects for the Higgs pseudoscalar resonance (A funnel), which provides another candidate for thermal dark matter. This involves the lightest neutralino (the bino) at approximately half the mass of the pseudoscalar Higgs boson A, resulting in an enhancement of the annihilation cross section through A exchange.[1] We note that it cannot be mostly wino, nor Higgsino, since annihilations are too efficient already, and the enhancement due to resonance would be detrimental; on the other hand, the annihilation cross section of a bino is generally too small, leading to overclosure of the Universe upon freeze-out, but the resonance enhancement facilitates the correct relic density. This is a fine-tuned region since the bino and A masses are generally not correlated; however, given the

*anandakrishnan.1@osu.edu
†bshakya@umich.edu
‡kusinha@syr.edu

[1]We note that resonances through Z, h, and H are also possible, but do not study these, since they predict larger direct detection cross sections in general. Dark matter at the Higgs resonance is currently constrained more strongly by Higgs invisible decays than by LUX [10,11]. XENON1T and LZ will significantly constrain this region. There will be complementary constraints in these cases from the LHC.

 © 2015 American Physical Society

increasingly stringent constraints from direct detection experiments, the pseudoscalar resonance constitutes one of the few remaining thermal dark matter candidates that can remain safe from such constraints.[2] Moreover, this is a region that can be attacked from multiple angles: new physics contributions to rare decays such as $B_s \to \mu^+\mu^-$ and LHC constraints on $A \to \tau\tau$ search [14,15] can constrain m_A. The combination of direct searches at the LHC, rare B-decay processes, and direct detection may therefore ultimately either validate or rule out this window.

We study the prospects of the pseudoscalar Higgs resonance from two different approaches. The first, in Sec. II, is from the bottom-up perspective of the phenomenological MSSM with parameters taken to be independent at the weak scale. This offers the opportunity to study the pseudoscalar resonance in isolation with a handful of parameters by decoupling all physics that does not affect it directly. This serves as a general framework within which more constrained models can be embedded. Such a model is studied in Sec. III in the framework of a Yukawa unified $SO(10)$ GUT model. $SO(10)$ GUTs are one of the economical choices for a grand unified theory and Yukawa unification is a natural feature of these models. In contrast to the pMSSM, a Yukawa unified GUT affords little freedom in its choice of parameters due to simultaneous constraints from fermion masses, flavor physics, and collider bounds.

The strikingly different characteristics of these two models illustrate some key aspects of the pseudoscalar resonance region. In both extremes, we look for complementary probes of the region and show that the next generation direct detection experiments will be aided by the LHC searches for supersymmetric particles.

II. RESONANCE REGION IN THE PMSSM

As described in the Introduction, the pseudoscalar resonance is an attractive possibility even in the generic MSSM. A detailed study of MSSM resonances was performed previously in [16,17]. We give projected reaches for upcoming direct detection experiments, examine particularly low cross sections and discuss complementarity with collider bounds and rare decays.

To focus on the relevant parameter space, we take a "decoupling approach," in the sense that any physics that does not contribute to the resonance, or constrains it, is made heavy enough to decouple from the analysis. Thus we take scalar masses to be uniformly heavy to block stau/stop coannihilation effects or t-channel scalar exchange. The wino mass is similarly taken to be much larger than the bino mass to block coannihilation effects. All these parameters are set to 5 TeV.

[2]We will consider only thermal candidates here. For non-thermal histories, several options remain open [12,13].

The remaining free parameters, which we scan over using `MicrOMEGAs` (3.6.9.2) [18], are

(i) Bino mass m_1: This is the mass of the dark matter candidate. We scan values between 100–1000 GeV. Although lower masses are possible, we focus on this range to avoid contamination with the Z and SM-like Higgs resonances, since our main goal is to study the A funnel. Note that the decoupling limit $m_A \gg m_Z$ holds in this regime.

(ii) Pseudoscalar mass m_A: $M_A \sim 2M_1$ is necessary to enforce the resonance; in our scans, the numbers are constrained to be within 10% of each other.

(iii) $\tan\beta$: Scanned between 2 and 50.

(iv) μ: Since coupling to the pseudoscalar requires a bino-Higgsino admixture, requiring the correct relic density fixes the value of μ [we require $\Omega h^2 \in (0.08, 2.0)$]. This occurs for values of $|\mu| \sim$ 1–10 TeV (see [16]), and this is our scan interval. While [16] only studied positive values of μ, we extend our scans to negative values as well.

In addition to the correct relic density, we also require the lightest Higgs mass to fall between 123–128 GeV. While this has no bearing on the neutralino sector or the relic density in the A funnel, it is necessary to correctly calculate the spin-independent direct detection cross section.

The results of our scan are presented in Fig. 1, which shows the spin-independent WIMP-nucleon (proton) scattering cross section σ_{SI} as a function of the LSP mass. Positive (negative) values of μ are plotted in red (black). With all scalars heavy, this cross section comes from light and heavy CP-even Higgs exchange in the t channel, facilitated by the bino-Higgsino mixture of the LSP that is necessary to obtain the correct relic density. There are also contributions from tree level squark exchange in the s channel and from gluon loops [19,20], but these are negligible when the superpartners are heavy. The three

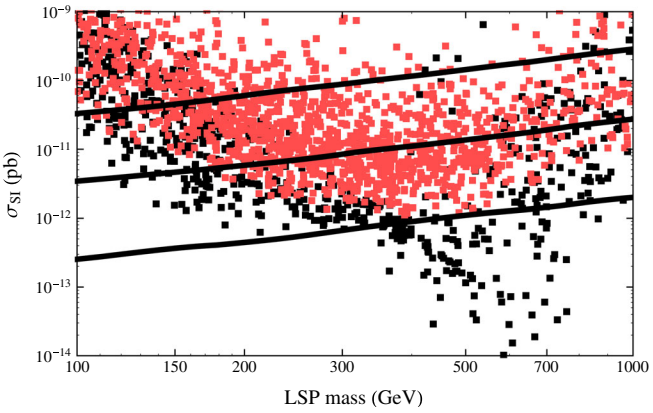

FIG. 1 (color online). Direct detection cross section as a function of LSP mass. Negative μ in black, positive in red. The three lines correspond to (top to bottom) the projected XENON1T reach, projected LZ reach, and the irreducible neutrino scattering background.

lines on the plot correspond to (top to bottom) the projected XENON1T reach, projected LZ reach, and the irreducible neutrino scattering background, respectively, taken from [21].

For positive values of μ (red points), the cross section is generally found to be around 10^{-11} pb, in agreement with the findings in [16,17,22]. Since the resonance requires only a tiny Higgsino fraction in the LSP to give the correct relic density, such small cross sections are a generic feature of this region of parameter space. While the cross sections are well below existing bounds from XENON-100 and LUX, they crucially all lie above the neutrino background and are, therefore, within reach of future detectors, although detection will still be challenging.

In contrast, for negative values of μ (black points), we find points with cross sections several orders of magnitude below the neutrino background cross section. This was also found in the study in [17]. As is well known, such low cross sections occur due to destructive interference between the light and heavy Higgs exchange contributions. Assuming equal couplings to up- and down-type quarks in the nucleus, the cancellation condition can be roughly formulated as [23]

$$\frac{m_H}{m_h} \sim \sqrt{-\frac{\mu}{m_\chi}\tan\beta}. \tag{1}$$

Since this contains precisely the same parameters we have scanned over, this therefore acts as an additional constraint in our parameter space. In the A-funnel setup, $m_H \sim m_A \sim 2m_\chi$, so this cancellation condition can be rewritten as

$$m_A \sim (-2\mu m_h^2 \tan\beta)^{1/3}. \tag{2}$$

For all points with cross sections below $\sim 5 \times 10^{-13}$ pb, where the cancellation is expected to be in effect, we find that this relation is indeed satisfied within a factor of 2. While a blind spot can in general occur at any LSP mass, its appearance in the case of the A funnel is therefore more strongly constrained. Requiring the right relic density further constrains a combination of μ and $\tan\beta$: the correct relic density is obtained for $\mu \sim 1$–10 TeV (see e.g. [16]). Together with Eq. (2), these conditions roughly require $m_A > 800$ GeV for the blind spot and the pseudoscalar resonance to occur simultaneously; this is indeed visible in Fig. 1.

Next, we study the scan results in the M_A-$\tan\beta$ plane. Figure 2 shows the points in this parameter space, color coded by cross section (see caption for details). There exist robust constraints on this parameter space from LHC searches of scalar Higgs boson decays in the $\tau\tau$ channel [14,15]; the black curve denotes the bound from CMS [15]. This rules out a significant chunk of parameter space, in particular pseudoscalar masses below ~300 GeV.

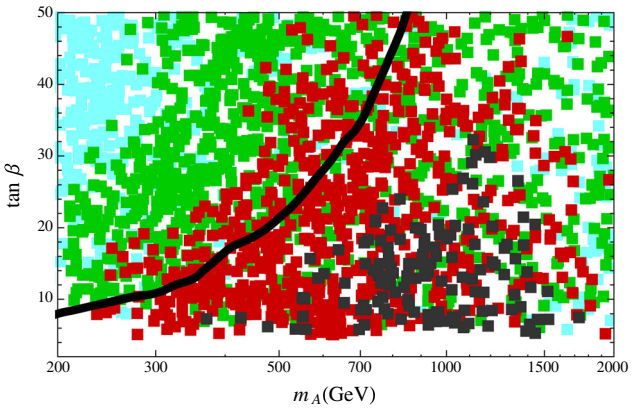

FIG. 2 (color online). Direct detection cross section color coded in the M_A-$\tan\beta$ plane. Cyan, green, red and black points correspond to $\sigma_{SI} \in (> 10^{-10}), (10^{-11}, 10^{-10}), (10^{-12}, 10^{-11}), (< 10^{-12})$ pb, respectively. The curve denotes the CMS bound from $H/A \to \tau\tau$ [15].

Nevertheless, above this mass, realization of the A funnel is fairly unconstrained. Future runs of the LHC as well as e^+e^- colliders will further constrain this parameter space (see [24] for projections). However, that the cross section tends to fall from left to right shows that points with progressively lower direct detection cross section are also progressively less likely to be ruled out by such searches at the LHC, since both get suppressed at heavier m_A. Nevertheless, cross sections sizable enough to be within reach of planned detectors can be realized in all regions of this parameter space, as evident from the presence of blue and green points all over the plot.

There are additional constraints from $B_s \to \mu^+\mu^-$ [25] and $B \to X_s\gamma$ [26,27], but these depend on additional parameters as well as flavor structures and can be evaded by judiciously choosing parameters in the scalar sector (see [28] for extensive discussions and scans). Constraints from metastability of the EW vacuum [29,30] are also important, but can likewise be avoided by properly choosing parameters. These, therefore, do not significantly constrain the A funnel in the pMSSM due to the freedom in choosing parameter values.

III. RESONANCE IN THE $SO(10)$ GUT MODEL

In this section, we consider the pseudoscalar resonance in the class of highly predictive Yukawa unified GUT models [31–41]. Compared to the pMSSM, we will see that requiring compatibility of the pseudoscalar Higgs resonance with constraints such as $B_s \to \mu^+\mu^-$ has nontrivial consequences.

A particularly appealing aspect of $SO(10)$ SUSY GUT models is the possibility of unifying all quarks and leptons of a given generation into a single 16 representation of the gauge group

$$W \supset \lambda 16_3 1016_3. \tag{3}$$

Third-generation Yukawa unification becomes a possibility for $\tan\beta \sim 50$. Yukawa couplings, however, are more sensitive than gauge couplings to weak scale threshold corrections; hence, this unification depends critically on the SUSY spectrum and other parameters. Under the assumption of universal scalar and gaugino masses and A terms at the GUT scale (m_{16}, $M_{1/2}$, and A_0, respectively),[3] Yukawa unification prefers a region of parameter space where the following relations hold:

$$-A_0 \sim 2m_{16}, \qquad \mu, m_{1/2} \ll m_{16}. \tag{4}$$

This region is preferred because large $\tan\beta$ corrections to the bottom quark mass are cancelled here as discussed below. Thus, one can already see that requiring Yukawa unification severely constrains the MSSM parameter space compared to the pMSSM study conducted in the previous section. We begin by reviewing the constraints on the parameter space of these models.

(1) *Heavy scalars with $m_{16} \geq 8$ TeV are required to suppress new physics contributions to $B \to X_s\gamma$.* The first measurements of the $\mathrm{BR}(B \to X_s\gamma)$ by the CLEO, Belle, and *BABAR* Collaborations [42] compelled the supersymmetric scalars to be heavy. Both $B^+ \to \tau^+\nu$ and $B \to X_s\gamma$ receive new physics contributions at large $\tan\beta$: the former from charged Higgs bosons through a term that interferes destructively with the SM contribution [43] and the latter from chargino-stop loop and top-charged Higgs loop diagrams [44]. The former is suppressed for decoupled Higgs partners and we will not consider it further since $B_s \to \mu^+\mu^-$ (discussed below) gives more stringent bounds. For $B \to X_s\gamma$, the chargino-stop loop term goes as $\sim \frac{\mu A_t}{\tilde{m}^2}\tan\beta$, where $\tilde{m}$ is a low-scale squark mass. For large $\tan\beta$ and large A_t satisfying Eq. (4), the universal scalar mass is required to be ≥ 8 TeV [39,45] in models with third-family Yukawa coupling unification.

(2) *$B_s \to \mu^+\mu^-$ constraints require $M_A \gtrsim 1200$ GeV.* The branching ratio of the decay $B_s \to \mu^+\mu^-$ receives large $\tan\beta$ enhanced contributions from Higgs-mediated neutral currents, proportional to $A_t^2(\tan^6\beta)/M_A^4$ [46]. The twin requirements of large $\tan\beta$ and A_t from Eq. (4) necessitate large masses for the Higgs cousins A^0, H^0, and H^+. With the measurement of the this rare decay branching ratio by the LHCb Collaboration [47], CP-odd Higgs mass larger than 1200 GeV are preferred by these models [39]. This puts a lower bound on the neutralino dark matter mass for the resonance to be operational.

(3) *Upper bound on gluinos ~2 TeV.* A spectrum in the Higgs decoupling limit and with heavy scalars is preferred in Yukawa unified $SO(10)$ when rare B decay constraints are taken into account. Moreover, the spectrum has an inverted mass hierarchy with third-family squarks and sleptons between 3–6 TeV. In addition, there are well known $\tan\beta$ enhanced corrections to the b quark mass:

$$\frac{\delta m_b}{m_b} \simeq \frac{g_3^2}{12\pi^2}\frac{\mu M_{\tilde{g}}\tan\beta}{m_{\tilde{b}}^2} + \frac{\lambda_t^2}{32\pi^2}\frac{\mu A_t\tan\beta}{m_{\tilde{t}}^2}. \tag{5}$$

In models with third-family Yukawa unification, the threshold corrections typically need to be $\mathcal{O}(\text{few})\%$ and negative. It is necessary that the two terms in Eq. (5) must both be suppressed or nearly cancel since the corrections from gluinos and charginos can independently be large. If gluinos are too heavy, this pushes A_t to large (negative) values, beyond maximal mixing, to fit the bottom quark mass. Good fits to the observed Higgs mass requires that the gluinos be light. For universal scalar masses $m_{16} < 20$ TeV, it was found that Eq. (5) implied an upper bound on the gluinos of 2 TeV [39]. This upper bound can be relaxed by increasing the universal scalar mass, at the expense of naturalness.

(4) *Light Higgsinos $\lesssim$500 GeV are disfavored.* Given that scalars have to be heavy, light Higgsinos further suppress the corrections in Eq. (5) below the nominally required value. In fact, a recent study by some of the authors [48] found that for $m_{16} = 20$ TeV, Higgsinos below $\lesssim$500 GeV are disfavored after the recent Higgs mass measurement. Note that negatives values of μ would be preferable for the expression in Eq. (5), and this choice has been studied in previous works [31], where it was found that the contributions to $B \to X_s\gamma$ are enhanced in such scenarios.

The above observations, taken together, have immediate consequences for thermal dark matter. In [48] the well-tempered neutralino was explored in this class of models, but found to be increasingly under tension from direct detection. Opting instead for the pseudoscalar resonance, (3) above implies an upper limit on the bino mass $M_1 \sim 300$ GeV (this follows from the familiar 1:2:6 mass ratio from gaugino mass unification). Therefore, points (2) and (3) imply that *pseudoscalar resonance dark matter requires nonuniversal gaugino masses.*

We note that this is a nontrivial prediction about the spectrum coming from the requirement of thermal dark matter. Point (1) forces a lower bound $m_{\tilde{\chi}_1^0} \gtrsim 600$ GeV on the dark matter particle, while point (4) makes it clear that the corresponding gluino must be more compressed than the universal case. The requirement of a compressed spectrum was natural in the case of well tempering, but

[3]We will explore mild departures from gaugino mass universality in our analysis.

we find that this requirement holds for the A-resonance region as well. We should note a small caveat to this conclusion. The upper bound on the gluino mass depends on the universal scalar mass m_{16}, as is clear from Eq. (5). For $m_{16} \sim 30$ TeV, the upper bound increases to $m_{\tilde{g}} \lesssim 2.8$ TeV. This is still a departure from universality, but less so. For sufficiently high scalar masses and heavy gluino, compatibility with universality may be restored, but such scenarios are not directly testable in the near future.

A. Estimate of gaugino mass ratios

In this subsection, we carry out a detailed χ^2 analysis to obtain a prediction for the gaugino mass ratio that is preferred by the pseudoscalar resonance.

Nonuniversality of gaugino masses is parameterized via an additional parameter in the gaugino sector, α. The boundary condition we choose for the gaugino masses is mixed modulus-anomalous (mirage) mediation [49–51], which is independently well motivated from string constructions. The gaugino masses at the GUT scale obey a "mirage" pattern:

$$M_i = \left(1 + \frac{g_G^2 b_i \alpha}{16\pi^2} \log\left(\frac{M_{Pl}}{m_{16}}\right)\right) M_{1/2}. \tag{6}$$

In the above expression, α controls the relative importance of the universal and anomalous contributions, and $b_i = (33/5, 1, -3)$ for $i = 1, 2, 3$ are the relevant β-function coefficients. $\alpha = 0$ corresponds to the universal gaugino mass scenario and larger α leads to larger anomaly-mediated contributions and a compressed gaugino spectrum. At $\alpha \gtrsim 3$, the gluino becomes the LSP and the spectrum is not viable. Larger $\alpha > 4$ can be accommodated by considering negative $M_{1/2}$ at the GUT scale and yields a wino LSP [40].

We calculate 12 low energy observables following the procedure outlined in Ref [40]. A global χ^2 analysis is performed with the observables $M_W, M_Z, G_F, \alpha_{\rm em}^{-1}$, $\alpha_s(M_Z), M_t, m_b(m_b), M_\tau$, $b \to s\gamma$, $\mathrm{BR}(B_s \to \mu^+\mu^-)$, and M_h. We then explore the best-fit regions and study the thermal relic abundance, Ωh^2.

The input parameters are as follows. There are the three gauge parameters, $\alpha_G, M_G, \epsilon_3$, where $\alpha_1(M_G) = \alpha_2(M_G) \equiv \alpha_G$, and $\epsilon_3 = \frac{\alpha_3 - \alpha_G}{\alpha_G}$ is the GUT scale threshold corrections to the gauge couplings. There is one large Yukawa coupling, λ, which satisfies $\lambda_t(M_G) = \lambda_b(M_G) = \lambda_\tau(M_G) = \lambda$.[4] The SUSY parameters defined at the GUT scale are m_{16}, $M_{1/2}$, A_0, the universal Higgs mass m_{10}, and the magnitude of Higgs splitting D. There is also the gaugino nonuniversality parameter α. Radiative electroweak symmetry breaking forces nonuniversal Higgs masses in these models.

We consider several different values of α, which will allow us to deviate from gaugino mass universality. For each α, we scan different values of $M_{1/2}$ and μ, in the range of $M_{1/2} = 500$–950 GeV, and $\mu = 800$–1300 GeV. We note that the A funnel can be realized to much higher values of μ, up to several TeV; however, we restrict ourselves to this range since it contains all the qualitatively interesting aspects that we wish to discuss, and higher values of μ do not introduce any new behavior. The value of M_A is kept within the range of 1200–1400 GeV.

We display our results in Fig. 3. The region between the red lines gives $\Omega h^2 = 0.08$–0.2. The olive contours give the spin-independent DM-nucleon scattering cross section. The scattering cross-section of the DM candidate depends strongly on the Higgsino component. This is evident from Fig. 3, where the scattering cross sections are the largest where the LSP is a bino/Higgsino mixture (in the top left corner of the plot) due to the proximity of the values of $M_{1/2}$ and μ. This region shows significantly high DM-nucelon scattering cross section and is ruled out by current data. The scattering cross section decreases as we go to the bottom right corner of the plot, as Higgsinos progressively become heavier and the bino/Higgsino mixing decreases. The four shades of blue contours (lightest to darkest) represent $\chi^2/\text{d.o.f.} < 1, 2.3, 3$, and greater respectively, corresponding to 95%, 90%, and 68% C.L.s. The darkest shade of blue are the worst fits and we essentially rule the spectrum out as a good solution.

The case of $\alpha = 0$ (universal gaugino masses) is disfavored and hence we do not plot it. In the top row of 3, we display the cases of $\alpha = 0.5$ and $\alpha = 1.0$. For the case of $\alpha = 0.5$ which is only a slight deviation from the universal scenario, the relic density corridor lies in the region with $\chi^2/\text{d.o.f.} > 2.3$ due to a heavy gluino and the Higgs mass is typically less than 120 GeV in this region. The fits become better as α increases, and we see this in the case of $\alpha = 1.0$, where the effect of lower gluino masses pushes the relic density corridor into the 90% confidence level region.

In the bottom left panel, we display the case of $\alpha = 1.5$, which is an optimal scenario. For the range of $M_{1/2}$ considered, the gluino mass is in a region that gives good fits to both the bottom mass and the Higgs mass. Thus, the entire figure has $\chi^2/\text{d.o.f.} \lesssim 1$. The relic density is satisfied in the region which has the pseudoscalar resonance, marked by $M_{1/2} \sim 500$–600 GeV. In the right panel, we display the case of $\alpha = 2.0$. In this case, the anomaly contributions start to dominate, and the LSP becomes predominantly wino. There is, thus, no relic density preferred region.

To summarize, we find two effects as we increase α. While $\alpha = 0$ does not accommodate good fits to all

[4]There are typically small corrections to this relation at the GUT scale, coming from the off-diagonal Yukawa couplings to the first two families. In this work, we will mainly consider a third-family model, since the details of small off-diagonal Yukawa couplings will not affect the supersymmetric spectrum or dark matter calculations.

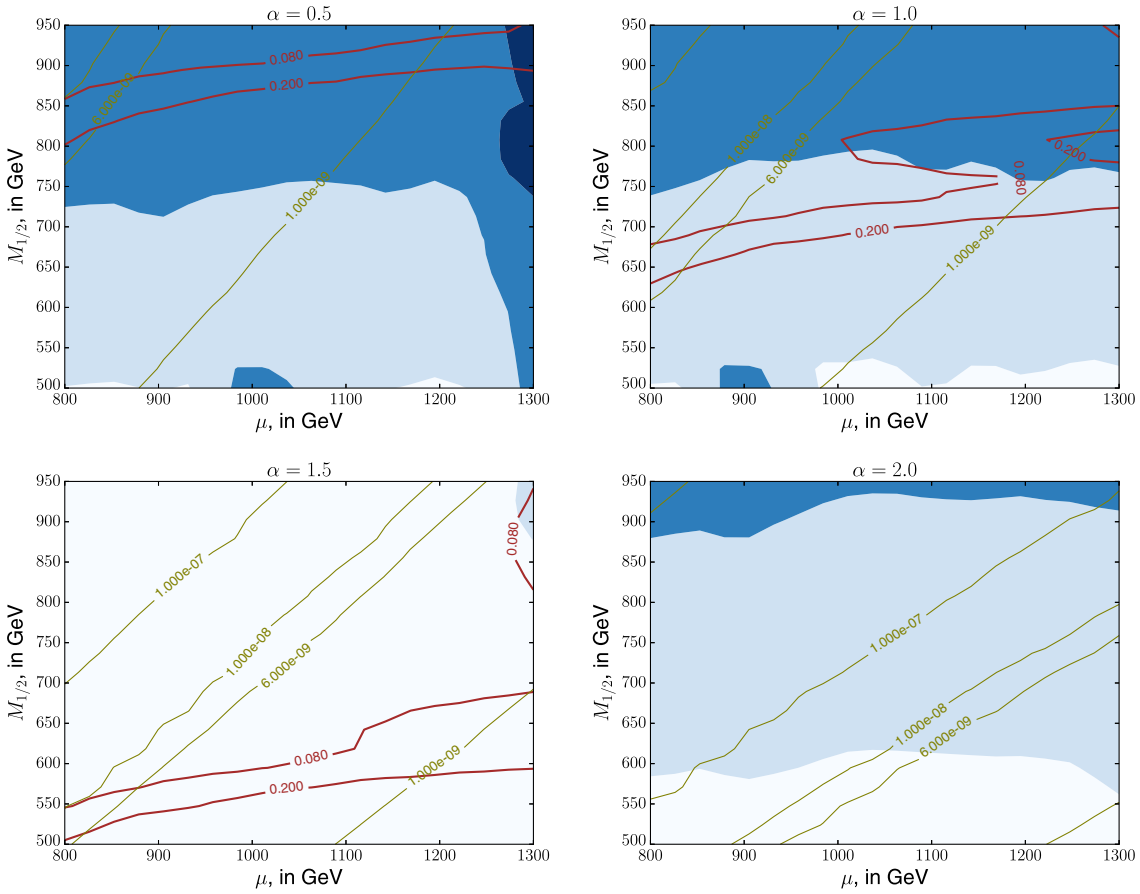

FIG. 3 (color online). Best-fit regions on a graph of $M_{1/2}$ versus μ in the case of $\alpha = 0.5, 1.0, 1.5$ and 2. The region between the red lines gives $\Omega h^2 = 0.08$–0.2. The olive contours represent the spin-independent DM-nucleon direct detection cross sections. The blue shaded regions (lightest to darkest) represent $\chi^2/\text{d.o.f.} = 1, 2.3, 3$ and greater.

observables in the A-resonance region, as α increases (i) the gaugino masses become more compressed and the gluino satisfies condition (4) above, and (ii) since the β-function coefficient of $U(1)_Y$ is large, the resonance is forced to occur at smaller values of $M_{1/2}$. The ideal α region occurs around 1.5, above which the wino component of the LSP becomes dominant and the gluino mass is also driven below the current LHC bounds. Around this value, we have the following estimate of the gaugino mass ratios at the weak scale:

$$M_{\text{bino}} : M_{\text{wino}} : M_{\text{gluino}} \sim 1 : 1.2 : 2.2. \tag{7}$$

The robustness of this ratio depends on the value of α, which we have demonstrated to be confined within a narrow range for the given selection of m_A and m_{16} on which our results are based. Increasing m_A with m_{16} fixed would require raising the bino mass, and hence raising α to compress the gaugino spectrum further to accommodate the upper bound on the gluino mass. Requiring the bino to remain the LSP is found to require that α cannot deviate too much from our optimal value of $\alpha = 1.5$. On the other hand, increasing m_{16} to large enough values may accommodate gaugino universality with $\alpha = 0$, but such scenarios are less testable, as mentioned before. The mass ratios in Eq. (7) are therefore reasonably robust within testable models.

In Table I, we display the spectrum and input parameters at a sample benchmark point. The bino is at $m_{\tilde{\chi}_1^0} \sim 666$ GeV, while $M_A = 1300$ GeV, implying that the pseudoscalar resonance is operational here. The rest of the spectrum is very similar to minimal Yukawa unified GUTs, with heavy scalars. The gaugino spectrum is compressed and the gluino remains the only (but a very strong) viable candidate for detection at the LHC. For direct detection prospects, we refer to 1. For collider prospects, we refer to [52,53]. We note that even the best-fit points have a Higgs mass around 120 GeV. The low Higgs mass combined with the nonobservation of gluino could necessitate pushing the scalars to heavier mass or eventually disfavor these models.

In the event of a gluino discovery at the next run of the LHC, Eq. (7) can be taken as a hint from the dark sector to aid in our quest for the remaining gaugino spectrum.

TABLE I. Spectrum at the benchmark point for A-funnel region from the Yukawa unified GUT scenario. The constrained parameter space allows one to determine the entire supersymmetric spectrum. All masses are in GeV and cross section in pb.

GUT scale	m_{16}	20408	$M_{1/2}$	650	A_0	−40656	α	1.5
parameters	m_{H_d}	27364			m_{H_u}	24147		
	$1/\alpha_G$	26.29	M_G	2.03×10^{16}	ϵ_3	0%	λ	0.585
EW parameters	μ	1300			$\tan\beta$	49.13		
Fit	Total χ^2	1.63						
Spectrum	$m_{\tilde{u}}$	∼20103	$m_{\tilde{d}}$	∼20203	$m_{\tilde{e}}$	∼20569		
	$m_{\tilde{t}_1}$	4126	$m_{\tilde{b}_1}$	5714	$m_{\tilde{\tau}_1}$	8296	$M_{\tilde{g}}$	1428
	$m_{\tilde{\chi}_1^0}$	666	$m_{\tilde{\chi}_2^0}$	770	$m_{\tilde{\chi}_3^0}$	1304	$m_{\tilde{\chi}_4^0}$	1309
	$m_{\tilde{\chi}_1^+}$	770			$m_{\tilde{\chi}_1^+}$	1309		
	M_A	1300	$M_H^\pm$	1302	M_H	1526	M_h	120
DM	Ωh^2	0.151			SI cross section		8.076×10^{-10}	
Dominant $\tilde{g}$ BR	$tb\tilde{\chi}_1^\pm$	61%	$t\bar{t}\tilde{\chi}_2^0$	26%	$t\bar{t}\tilde{\chi}_1^0$	8%	$b\bar{b}\tilde{\chi}_1^0$	2%

IV. DISCUSSION

Given the freedom of the pMSSM, the A funnel is readily realized. The spin-independent direct detection cross section is well below current bounds, and the only robust experimental constraint is the heavy neutral Higgs bound from the LHC [14,15]. There is enough freedom in other sectors of the theory to evade robust bounds from current constraints on B decays. On the direct detection front, a significant chuck of the pseudoscalar resonance region in the pMSSM will be ruled out by the projected reach of XENON1T and especially LZ (see 1). For $\mu > 0$, the entire parameter space for $100\ \text{GeV} < m_{\tilde{\chi}_1^0} < 1000\ \text{GeV}$ lies above the coherent neutrino background, so experiments in the future will in principle be able to rule out the resonance. For $\mu < 0$, cancellations can lower the scattering cross section below the coherent neutrino background; however, such cancellations are constrained to a small subset of the parameter space above $m_A > 800$ GeV, enforced by additional requirements of the resonance and relic density.

In the far more constrained Yukawa unified $SO(10)$ GUT models, the story is very different. Unlike the pMSSM, the theory is forced to large values of $\tan\beta$, where the bound on m_A from $B_s \to \mu^+\mu^-$ becomes extremely strong. Fits to b-quark and Higgs masses and gluino mass bounds from the LHC then make it impossible to realize the A funnel for universal gauging masses, necessitating nonuniversality.

The two models therefore paint very different pictures of a thermal dark matter candidate via the pseudoscalar resonance in a supersymmetric model. In the pMSSM, bino annihilating through the A funnel is a readily available thermal dark matter candidate largely safe from current experimental constraints (and in the case of $\mu < 0$, can lie below the neutrino background for direct detection), and largely decoupled from the remainder of the supersymmetric spectrum. In the GUT model, there are extremely strong constraints, but consequently the theory has predictive power. We performed a detailed χ^2 analysis to determine the required degree of nonuniversality of gauging masses and presented the gaugino mass ratios at the weak scale. The gluino is a very strong candidate for detection at the LHC in this class of models; in the event of such a discovery, these mass ratios could serve as a prediction of the bino and wino masses if the pseudoscalar resonance is indeed responsible for the observed dark matter density.

ACKNOWLEDGMENTS

We acknowledge useful conversations with Stuart Raby and Nausheen Shah. We also thank the Mitchell Institute at Texas A&M, where part of this work was completed, for hospitality. A. A. is supported by the Ohio State University Presidential Fellowship. A. A. also thanks the hospitality of CLASSE, Cornell University, where a major portion of this work was completed. B. S. is supported by the U.S. DOE under Contract No. DE-SC0007859. K. S. is supported by a NASA Astrophysics Theory Grant No. NNH12ZDA001N.

[1] E. Aprile *et al.* (XENON100 Collaboration), Phys. Rev. Lett. **109**, 181301 (2012).
[2] D. S. Akerib *et al.* (LUX Collaboration), Phys. Rev. Lett. **112**, 091303 (2014).
[3] N. Arkani-Hamed, A. Delgado, and G. F. Giudice, Nucl. Phys. **B741**, 108 (2006).
[4] M. Perelstein and B. Shakya, Phys. Rev. D **88**, 075003 (2013).
[5] M. Perelstein and B. Shakya, J. High Energy Phys. 10 (2011) 142.
[6] R. Easther, R. Galvez, O. Ozsoy, and S. Watson, Phys. Rev. D **89**, 023522 (2014).
[7] R. Allahverdi, B. Dutta, and K. Sinha, Phys. Rev. D **86**, 095016 (2012).
[8] T. Cohen, M. Lisanti, A. Pierce, and T. R. Slatyer, J. Cosmol. Astropart. Phys. 10 (2013) 061.
[9] J. Fan and M. Reece, J. High Energy Phys. 10 (2013) 124.
[10] F. S. Queiroz, K. Sinha, and A. Strumia, Phys. Rev. D **91**, 035006 (2015).
[11] F. S. Queiroz and K. Sinha, Phys. Lett. B **735**, 69 (2014).
[12] B. Dutta, L. Leblond, and K. Sinha, Phys. Rev. D **80**, 035014 (2009).
[13] R. Allahverdi, B. Dutta, and K. Sinha, Phys. Rev. D **83**, 083502 (2011).
[14] G. Aad *et al.* (ATLAS Collaboration), J. High Energy Phys. 11 (2014) 056.
[15] CMS Collaboration, Report No. CMS-PAS-HIG-13-021.
[16] D. Hooper, C. Kelso, P. Sandick, and W. Xue, Phys. Rev. D **88**, 015010 (2013).
[17] T. Han, Z. Liu, and A. Natarajan, J. High Energy Phys. 11 (2013) 008.
[18] G. Belanger, F. Boudjema, A. Pukhov, and A. Semenov, Nuovo Cimento Soc. Ital. Fis. **033N2**, 111 (2010).
[19] J. Hisano, K. Ishiwata, and N. Nagata, Phys. Rev. D **82**, 115007 (2010).
[20] C. Cheung, L. J. Hall, D. Pinner, and J. T. Ruderman, J. High Energy Phys. 05 (2013) 100.
[21] P. Cushman, C. Galbiati, D. N. McKinsey, H. Robertson, T. M. P. Tait, D. Bauer, A. Borgland, and B. Cabrera *et al.*, arXiv:1310.8327.
[22] Y. G. Kim, T. Nihei, L. Roszkowski, and R. Ruiz de Austri, J. High Energy Phys. 12 (2002) 034.
[23] J. L. Feng and D. Sanford, J. Cosmol. Astropart. Phys. 05 (2011) 018.
[24] I. M. Lewis, arXiv:1308.1742; E. Brownson, N. Craig, U. Heintz, G. Kukartsev, M. Narain, N. Parashar, and J. Stupak, arXiv:1308.6334; A. Djouadi and J. Quevillon, J. High Energy Phys. 10 (2013) 028; S. Dawson, A. Gritsan, H. Logan, J. Qian, C. Tully, R. Van Kooten, A. Ajaib, A. Anastassov *et al.*, arXiv:1310.8361.
[25] A. Arbey, M. Battaglia, F. Mahmoudi, and D. Martinez Santos, Phys. Rev. D **87**, 035026 (2013).
[26] M. S. Carena, D. Garcia, U. Nierste, and C. E. M. Wagner, Phys. Lett. B **499**, 141 (2001).
[27] K. Ishiwata, N. Nagata, and N. Yokozaki, Phys. Lett. B **710**, 145 (2012).
[28] W. Altmannshofer, M. Carena, N. R. Shah, and F. Yu, J. High Energy Phys. 01 (2013) 160.
[29] A. Kusenko, P. Langacker, and G. Segre, Phys. Rev. D **54**, 5824 (1996).
[30] J. A. Casas, A. Lleyda, and C. Munoz, Nucl. Phys. **B471**, 3 (1996).
[31] T. Blazek, R. Dermisek, and S. Raby, Phys. Rev. Lett. **88**, 111804 (2002).
[32] H. Baer and J. Ferrandis, Phys. Rev. Lett. **87**, 211803 (2001).
[33] T. Blazek, R. Dermisek, and S. Raby, Phys. Rev. D **65**, 115004 (2002).
[34] K. Tobe and J. D. Wells, Nucl. Phys. **B663**, 123 (2003).
[35] D. Auto, H. Baer, C. Balazs, A. Belyaev, J. Ferrandis, and X. Tata, J. High Energy Phys. 06 (2003) 023.
[36] I. Gogoladze, Q. Shafi, and C. S. Un, Phys. Lett. B **704**, 201 (2011).
[37] I. Gogoladze, Q. Shafi, and C. S. Un, J. High Energy Phys. 08 (2012) 028.
[38] M. Badziak, M. Olechowski, and S. Pokorski, J. High Energy Phys. 08 (2011) 147.
[39] A. Anandakrishnan, S. Raby, and A. Wingerter, Phys. Rev. D **87**, 055005 (2013).
[40] A. Anandakrishnan and S. Raby, Phys. Rev. Lett. **111**, 211801 (2013).
[41] M. Adeel Ajaib, I. Gogoladze, Q. Shafi, and C. S. Un, J. High Energy Phys. 07 (2013) 139.
[42] Y. Amhis *et al.* (Heavy Flavor Averaging Group (HFAG) Collaboration), arXiv:1412.7515.
[43] W. S. Hou, Phys. Rev. D **48**, 2342 (1993); A. G. Akeroyd and S. Recksiegel, J. Phys. G **29**, 2311 (2003).
[44] G. Degrassi, P. Gambino, and G. F. Giudice, J. High Energy Phys. 12 (2000) 009; M. S. Carena, D. Garcia, U. Nierste, and C. E. M. Wagner, Phys. Lett. B **499**, 141 (2001).
[45] M. Albrecht, W. Altmannshofer, A. J. Buras, D. Guadagnoli, and D. M. Straub, J. High Energy Phys. 10 (2007) 055.
[46] A. J. Buras, P. H. Chankowski, J. Rosiek, and L. Slawianowska, Nucl. Phys. **B659**, 3 (2003); S. R. Choudhury and N. Gaur, Phys. Lett. B **451**, 86 (1999); K. S. Babu and C. F. Kolda, Phys. Rev. Lett. **84**, 228 (2000).
[47] R. Aaij *et al.* (LHCb Collaboration), Phys. Rev. Lett. **110**, 021801 (2013).
[48] A. Anandakrishnan and K. Sinha, Phys. Rev. D **89**, 055015 (2014).
[49] K. Choi and H. P. Nilles, J. High Energy Phys. 04 (2007) 006.
[50] V. Lowen and H. P. Nilles, Phys. Rev. D **77**, 106007 (2008).
[51] H. Baer, E. K. Park, X. Tata, and T. T. Wang, Phys. Lett. B **641**, 447 (2006).
[52] A. Anandakrishnan, B. C. Bryant, S. Raby, and A. Wingerter, Phys. Rev. D **88**, 075002 (2013).
[53] A. Anandakrishnan, B. C. Bryant, and S. Raby, Phys. Rev. D **90**, 015030 (2014).